

SINERGI Vol. 29, No. 3, October 2025: 625-632 http://publikasi.mercubuana.ac.id/index.php/sinergi http://doi.org/10.22441/sinergi.2025.3.006



Experimental investigation of HHO blending in combustion engine performance



Awaludin Martin, Abda Hidayatullah, Yogie Rinaldy Ginting, Annisa Wulan Sari* Department of Mechanical Engineering, University of Riau, Indonesia

Abstract

The transition to renewable energy sources has become increasingly critical due to the adverse effects of greenhouse gas emissions. One alternative to reducing fossil fuel dependence is hydrogen. Hydrogen technology can be integrated into internal combustion engines without major design modifications. This study investigates the effects of HHO gas blending on engine performance under varying brake load conditions. The carburetor was modified to allow HHO gas from electrolysis to enter the combustion chamber. The results indicate that HHO blending led to a 4.9% increase in brake power, a 1.66% improvement in thermal efficiency, and a 3% reduction in brake-specific energy consumption (BSEC). Additionally, among different potassium hydroxide (KOH) concentrations, the 30% wt solution exhibited the lowest power consumption for electrolysis.

This is an open-access article under the CC BY-SA license.

Corresponding Author:

Annisa Wulan Sari Mechanical Engineering Department, Universitas Riau, Indonesia

Received: September 24, 2024

Revised: January 23, 2025

Accepted: February 17, 2025

Published: September 2, 2025

Email:

Keywords: Electrolysis;

Hydrogen;

Performance;

Article History:

Internal Combustion;

annisasw@lecturer.unri.ac.id



INTRODUCTION

The increasing concentration of greenhouse gases has contributed to rising global temperatures [1, 2, 3]. In response, various nations have committed to limiting temperature increases to below 1.5°C and achieving net-zero emissions by 2050, as outlined in the COP26 agreement. Reducing fossil fuel usage is imperative to achieving these targets, and hydrogen is a promising alternative due to its high energy density and clean combustion properties [4, 5, 6].

In order to achieve these targets, fossil energy reduction must be implemented globally by all stakeholders. An alternative renewable energy in reducing the use of fossil fuels is hydrogen [5][6]. Hydrogen as a fuel produces heat and water as emissions. The heating value of hydrogen gas is about 142.18 MJ/Kg (HHV) and 120 MJ/Kg (LHV) at 25°C [7]. The value of hydrogen is much higher than other fuels. Table 1 provides the significant differences characteristics between hydrogen and other fuels, highlighting the advantages of hydrogen gas.

Table 1. Comparison of Hydrogen, Gasoline, and Diesel Properties [8]

aa =					
Properties	H ₂	Gasoline	Diesel		
Auto-ignition temperature (K)	853	623	523		
Laminar lame speed (m/s)	4-76	0,3-0,4	0,3-0,4		
AFR (kg/kg)	34,4	14,7	14,5		
Lower Heating value (mJ/kg)	119,9	43,9	42,5		

Hydrogen can be produced through several methods, including hydrocarbon reforming (grey hydrogen), carbon capture-enhanced reforming (blue hydrogen), biomass processing, and electrolysis powered by renewable energy (green hydrogen) [9][10].

Electrochemical water electrolysis is a commonly used method for producing environmentally friendly hydrogen gas. This process involves applying direct current (DC) electricity to break the bond energy of water molecules, separating them into hydrogen and oxygen elements with a purity of up to 99.99% [7].

The chemical reactions involved in the electrolysis process are as follows [12]:

Reaction =
$$2H_2O_{(1)} \rightarrow 2H_{2(g)} + O_{2(g)}$$
 (1)

Anode =
$$2H_2O_{(1)} \rightarrow O_{2(q)} + H^+_{(aq)} + 4e^-$$
 (2)

Katode =
$$4H^{+}_{(aq)} + 4e^{-} \rightarrow 2H_{2(q)}$$
 (3)

Under standard conditions, the enthalpy (ΔH) of water is 285.85 kJ/mol, as calculated using the following equation:

$$2H_2O_{(I)} \rightarrow 2H_{2(g)} + O_{2(g)} \Delta H = 285,85 \text{ kJ/mol}$$
 (4)

 ΔH is the sum of:

$$\Delta H = \Delta G + T \Delta S \tag{5}$$

Where

$$\Delta G = 237,13 \text{ kJ/mol}$$
 (6)

$$T\Delta S = 48.72 \text{ kJ/mol} \tag{7}$$

Gibs free energy (ΔG) in electrolysis is the minimum energy required for the electrolysis reaction. The minimum voltage (E_{rev}) can be calculated through the following equation:

$$\mathsf{E}_{\mathsf{Rev}} = \frac{\Delta G}{z,F} = 1,23 \, \mathsf{V} \tag{8}$$

At the same time, energy input during the electrolysis process influences temperature (T) and entropy (ΔS). Consequently, the minimum voltage (V_{TN}) required for the electrolysis process under standard conditions is determined by the following equation:

$$V_{TN} = \frac{\Delta H}{z.F} = 1,48 \text{ V}$$
 (9)

F is Faraday's constant (F=96485 C/mol), and z is the number of electrons (2 for hydrogen and 4 for oxygen). In practice, the voltage required for electrolysis exceeds the theoretical minimum because of overpotential caused by resistive losses, reaction kinetics, gas pressure, electrode conductivity, electrolyte conductivity, distance between electrodes, and gas bubbles on the electrode surface [13].

The theoretical volume of hydrogen production is determined using the following equation [14]:

$$V_{H_2ideal} = \frac{i \cdot V_m \cdot t}{2 \cdot F} \tag{10}$$

Where V_{H_2ideal} is the theoretical volume of hydrogen, i is the current strength (A), t is the time (s), and F is Faraday's constant (96.485 C/mol). V_m is the molar volume.

An internal combustion engine can blend hydrogen without requiring significant modifications to its design. Blending hydrogen gas with fossil fuels improves combustion efficiency by reducing energy losses [15]. It also enhances

flame ignition properties and improves the combustion characteristics of hydrocarbon fuels [16]. Hydrogen plays a key role in reducing exhaust emissions from the transportation sector. The global vehicle count is projected to reach 1.6 billion by 2035, continuing to consume fossil fuels and emit pollutants that contribute to greenhouse gas emissions [17]. Therefore, hydrogen offers a practical approach to accelerating the energy transition while maintaining economic activity [18].

Gad et al. [19] utilized electrolyzed gas at 0.5 LPM, mixed with gasoline engine combustion at 3000 rpm. This study showed an increase in volumetric efficiency, thermal efficiency, and airfuel ratio by 7.5%, 8%, and 11%, respectively, reduced SFC by 9%, and reduced CO, HC, NOx, and CO₂ production by 18%, 9%, 15%, and 11%, respectively. Purayil et al. [20] tested a single-slider spark ignition engine with variations of 5 mg to 6 mg of gasoline and variations of hydrogen between 2, 5, 8, 11, and 14 LPM. This study showed that hydrogen gas at a flow rate of up to 11 LPM significantly reduces brake-specific energy consumption (BSEC) by 92.27% and increases BTE by 25%.

Hassan et al. [21] used a spark ignition engine with a capacity of 183 cc to mix hydrogen gas at 1500 rpm engine speed. The results showed an increase in engine efficiency by up to 47.24%, reduced BSEC by up to 32.1%, reduced CO production by up to 91.7%, and reduced HC by up to 34.84%. Adaileh and al Qdah [22] investigated the effects of using 3 LPM Hydrogen-Hydrogen oxygen (HHO) gas. The results showed an increase in adequate shaft power from 1198.2 watts to 1413 watts. Specific Fuel Consumption (SFC) decreased from 968 g/kW to 792 g/kW, and BTE improved from 16.93% to 23.48%. Furthermore, The HC emissions decreased from 240 ppm to 215 ppm.

Assad and Penazkov [23] showed that the concentration of hydrogen in mixing fuel and air could reach 20% of the total air entering the cylinder. This study also showed that using up to 20% of hydrogen increased the pressure in the combustion chamber by 19% to reach 5.8 Mpa, and the temperature in the combustion chamber increased by 140 K.

Based on the literature, HHO gas has proven to be a promising fuel for internal combustion engines. Previous studies have focused on understanding the effects of blending HHO in combustion engines, examining various parameters such as HHO flow rates, engine speed, and cylinder capacity [19, 20, 21, 22]. However, further analysis is still needed to evaluate the impact of HHO addition on engine performance under varying load conditions.

This study aims to investigate the effects of HHO blending on engine performance under varying brake loads, focusing on parameters such as brake power (BP), brake-specific energy consumption (BSEC), and brake thermal efficiency (BTE).

METHOD Hydrogen Electrolyzer Setup

The electrolyzer design in this study, which was developed and finalized prior to the commencement of the experiments, is detailed in Table 2, highlighting the pre-determined arrangement of components such as the electrodes, neutral plates, and electrolyte flow system to ensure compatibility with the research objectives and operational conditions.

The illustration of the electrolyzer are provided in Figure 1. The stack consists of 2 cells, each containing one anode plate (positive) and one cathode plate (negative), one neutral plate (not electrified) between the anode and cathode with a distance of 3 mm from each plate. Each plate is made of stainless steel 316 due to its high corrosion resistance and durability in alkaline solutions, while the neutral plate serves to minimize electrical interference between the anode and cathode.

The power source was a 12V 60Ah battery. A 12V 60Ah battery supplied power, with current variations of 30A, 40A, and 50A applied for each KOH concentration (20% wt, 25% wt, and 30% wt). The gas production rate and power consumption were measured using a flow meter and a wattmeter.

Based on these evaluations, the electrolysis tests revealed that the average gas production rates at current strengths of 30A, 40A, and 50A were 0.25 L/min, 0.3 L/min, and 0.4 L/min, respectively. Therefore, the electric power consumption for all currents at each molarity variation was recorded using a wattmeter.

Table 2. Specification of Electrolyzer

Parameters	Description
Type of Electrolyzer	Wett Cell
Type of Electrode	Stainless Steel 316
Dimension of Elektroda	1 mm X (10 X 10) cm
Number of cells	14
Number of stacks	7
Number of neutral plates	7
Capacity of electrolyzer	1 Liter

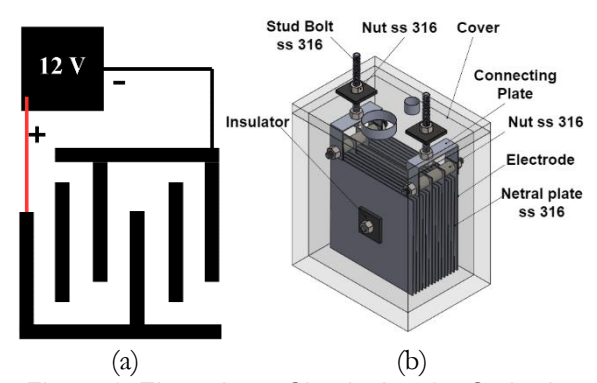


Figure 1. Electrolyzer Circuit: Anode, Cathode, and Neutral Plate (a), Electrolyzer Parts (b)

Experimental Procedure

The experiments were conducted in the Energy Conversion Laboratory at the University of Riau. Figure 2 illustrates the schematic of the experimental setup used in this study. The flow rate of the gas was measured using a flow meter. The gas was then transported through a pipe, blended with air, and directed into the intake manifold via the carburetor.

The engine used in this experiment was a three-cylinder, four-stroke gasoline engine, as detailed in Table 3. The fuel used was gasoline with an octane rating of 90, commonly known as Pertalite. The experiment began when the engine speed reached 2200 rpm, at which point the generated HHO gas was directed into the carburetor through a pipeline. A flashback arrestor was installed for safety. Brake loading was varied at 0.25 kg/cm², 0.5 kg/cm², and 0.75 kg/cm². The engine speed and fuel consumption time were recorded using a tachometer and a stopwatch while consuming 5 ml of fuel.

The first experiment began with gas generated from a 30A current at 20%wt KOH, which produced 0.25 LPM HHO gas, and the brake load was set at 0.25 kg/cm². Since the engine was operated under variations in the brake loading and KOH molarity, the effects of gas addition on engine performance were analyzed using the following parameters

Table 3. Specification of Gasoline Engine

Description
3-cylinder, four-stroke
3
993 cc
0.5:1
'6 mm x 73 mm
34.59 kW/ 5600 RPM
75.5 Nm/3200
֡

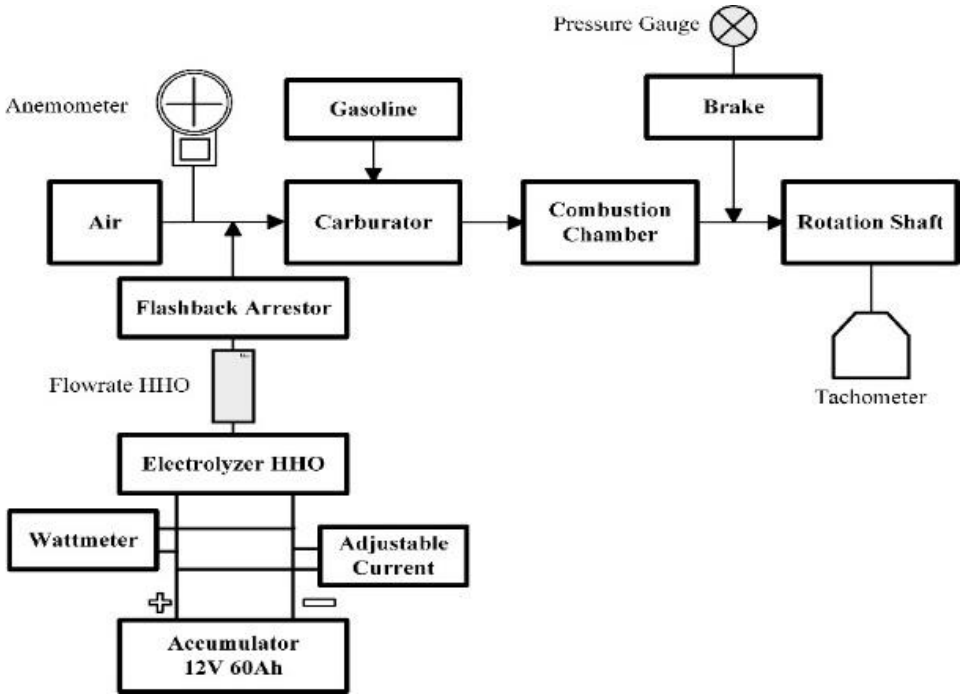


Figure 2. Schematic Experimental Setup

The effects of HHO blending were analyzed by evaluating BP, BSEC, and BTE, calculated using the following equations:

$$BP = \frac{T.2.\pi.n}{60} (W)$$
 (10)

BSEC =
$$\frac{(\dot{m}_{g.\ LHV_g} + \dot{m}_{H2.\ LHV_{H2}})}{Ne}$$
 (J/w)

$$BTE = \frac{Ne}{(\dot{m}_{g.\ LHV_g} + \dot{m}_{g.\ LHV_{H_2}})} \times 100 \text{ (\%)}$$
 (12)

RESULTS AND DISCUSSION

This experiment consists of two stages. In the first stage, the electrolyzer generates HHO gas by varying the current and molarity of potassium hydroxide (KOH). During this stage, the average HHO production and electricity consumption were measured by a flowmeter and a wattmeter. In the second stage, the HHO gas and air mix in the combustion engine. The HHO flow rate used was the average data obtained from the first stage. Then, the engine performance was analyzed by comparing the performance before and after blending HHO gas.

Energy Consumption for HHO

According to Ohm's law, a higher potential difference (voltage) results in a greater flow of current, facilitating the conduction of free ions. However, resistance within the system—such as that in the electrodes, electrolytes, and reaction container—causes a decrease in the input electric

current after passing through the electrolysis circuit. The voltage and current flowing through the system directly impact power consumption. Therefore, if power consumption is not proportional to hydrogen production, the process will not be economically efficient [24].

Variations in current strength of 30A, 40A, and 50A were tested for each molarity of KOH (20%wt, 25%wt, and 30%wt). Based on electrolysis tests in each variation in KOH molarity, the average gas production rate at current strengths of 30A, 40A, and 50A was 0.25 LPM, 0.3 LPM, and 0.4 LPM, respectively. The test also showed that to achieve these gas flow rates, the electric power consumption decreased by 30%wt KOH electrolyte compared to 25%wt and 20%wt KOH.

Figure 3 indicates that the electrical power consumption decreases as the molarity of KOH increases. The phenomenon is explained by the catalytic properties of KOH, which accelerate reaction kinetics and reduce water resistance. Lower resistance allows more ions per unit of time to separate H₂O into its elements [25][26]. At a KOH concentration of up to 30%wt, the specific electrolyte conductivity is significantly higher compared to lower concentrations. Higher conductivity reduces the voltage required for the electrolysis process. As a result, power consumption decreases, improving the electrolyzer's efficiency in producing the same amount of gas [27].

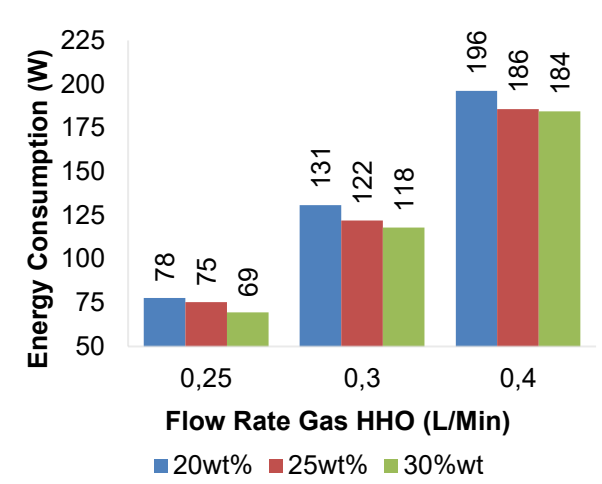


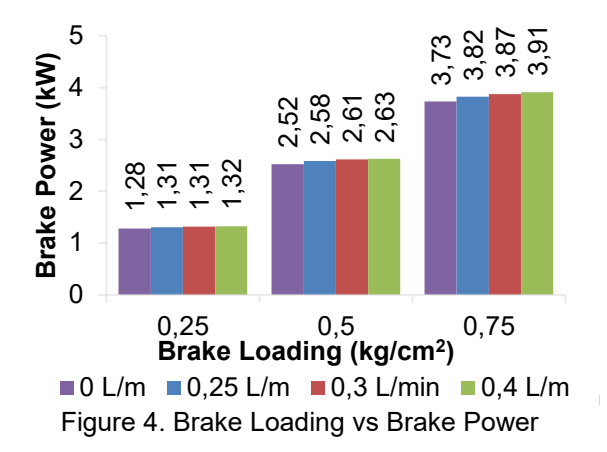
Figure 3. Energy Consumption vs Flowrate Gas HHO

The Effects of HHO Gas on the Internal Combustion Engine

As brake loading increases, the engine generates higher torque to maintain stable operation. The demand for higher torque leads to increased fuel consumption, which subsequently raises brake power output. The trend observed in Figure 4 illustrates the relationship between brake power and brake loading. At lower brake loading levels, the increase in brake power is relatively modest due to the lower torque demand. However, at higher loading levels, the increase becomes more significant.

Figure 4 shows the addition of varying HHO flow rate, blended in the combustion chamber, under different brake loading conditions. The addition of HHO enhances the brake power output at the same brake loading levels. The improvement occurs because the HHO gas acts as an auxiliary fuel, improving the engine performance by enhancing the flame speed and helping the fuel burn more completely. This leads to a more efficient energy conversion, which directly contributes to the observed increase in brake power.

In this experiment, the most significant increase in brake power, up to 4.9%, occurs when the brake load is 0.75 kg/cm², increasing from 3.73 kW to 3.91 kW with the addition of 0.4 LPM HHO. Nabil et al. [28], also observed an increase in brake power using HHO flow rates of 0.47 LPM to 0.51 LPM. Their results showed a brake power increase of up to 17.9% in a 150 CC engine and 22.4% in a 1300 CC engine. The difference in brake power gain was influenced by variations in engine capacity and rotation speed, which determine the amount of HHO burned during each combustion cycle. An increase in brake power indicates improved engine performance.

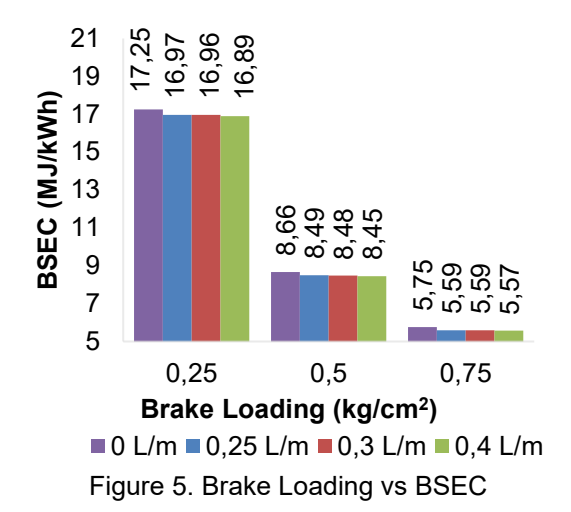


Brake-specific energy consumption (BSEC) was analyzed by observing the fuel consumption required to generate brake power. Higher brake loading results in reduced fuel consumption because the engine speed decreases, which in turn reduces the amount of fuel injected into the combustion chamber. A decrease in fuel consumption to generate a brake power at the same brake loading indicates improved efficiency.

Figure 5 shows the effect of all variations of HHO blending under varying brake loading conditions on the BSEC. The experiment shows that HHO blending reduces fuel consumption under all brake load conditions, with the most significant reduction observed in BSEC, up to 3%, occurring at a brake load of 0.25 kg/cm² with an HHO flow rate of 0.4 LPM; the decrease is from 5.75 MJ/kWh to 5.57 kWh.

A similar trend in BSEC reduction was also reported by Purayil et al. [20], who used hydrogen flow rate variations of 2, 5, 8, 11, and 14 LPM. The most significant BSEC reduction was obtained from 47.5 Mj/kWh to 3.7 MJ/kWh, representing a 92% decrease at a hydrogen flow rate of 11 LPM. The same result was also obtained by Gad et al. [19]. This study used 0.5 LPM HHO, with A decrease in specific fuel consumption (SFC) by up to 9%.

The reduction in BSEC observed in the experiment can be attributed to the unique combustion characteristics of HHO gas. Its high diffusivity enables homogeneous mixing with air in the combustion chamber [29], while its high flammability and heating value accelerate the combustion process, enhancing energy release [6][30]. Additionally, its high burning speed shortens the combustion duration, optimizing the conversion of thermal energy into mechanical work. These properties collectively improve the combustion efficiency of the air-fuel mixture, as evidenced by the reduction in fuel consumption observed in this study [31].



Thermal efficiency was also evaluated in this study, with the results presented in Figure 6. The findings indicate that thermal efficiency improves with increasing brake loading. As brake load increases, the engine operates closer to its optimal efficiency range, where a larger proportion of combustion energy is converted into useful work. This reduces the relative impact of frictional and thermal losses on total energy output.

The results also show that thermal efficiency increases with higher HHO gas flow rates. This improvement can be attributed to the combustion characteristics of HHO gas. The hydrogen content in HHO has a high burning speed, enabling faster and more complete combustion of the primary fuel. Additionally, the homogeneous mixing of HHO with air ensures an optimal air-fuel mixture, minimizing unburned hydrocarbons and reducing energy losses. Consequently, the conversion of chemical energy into mechanical work is enhanced, leading to increased thermal efficiency.

The experiment demonstrates the potential of HHO gas to improve thermal efficiency without requiring significant modifications to engine design under varying brake load conditions. It provides a more straightforward approach to emission reduction compared to other green energy solutions, such as electric vehicles. The use of hydrogen presents a practical pathway for the energy transition accelerating maintaining economic activity. Therefore, it offers immediate solution to reducing consumption and lowering emissions at an early stage.

The highest improvement in thermal efficiency, up to 1,66%, was achieved at an HHO flow rate of 0.4 LPM and a brake load of 0.75 kg/cm 2 . The result showed that efficiency increased from 63.37% to 65%.

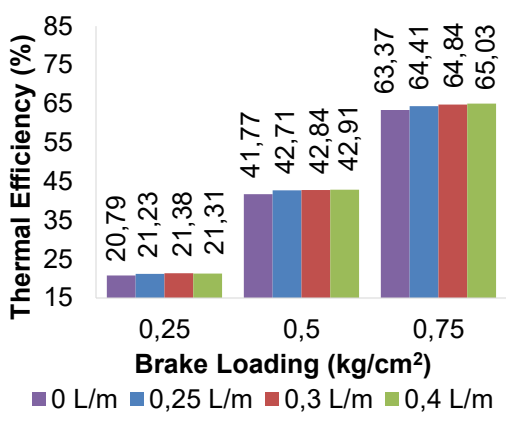


Figure 6. Brake Loading vs Thermal Efficiency

Although the improvements observed in this study are less significant than those reported by Gad et al. [19] (an 8% increase in thermal efficiency with 0.5 LPM HHO in a single-cylinder engine) and Adaileh & Al Qdah [22] (an increase in BTE from 16.93% to 23.48% with 3 LPM HHO in a four-cylinder engine). They provide valuable insights into the effects of HHO blending in multicylinder engines using a relatively lower HHO flow rate. This relatively modest improvement suggests that the effectiveness of HHO is influenced not only by its flow rate but also by engine configuration and combustion characteristics.

The data in Table 4 shows that the improvement of engine performance does not necessarily scale linearly with HHO flow rate. For example, while Hassan et al. [21] achieved a 47.24% increase in efficiency with only 0.2 LPM HHO in a single-cylinder engine. The present study of 0.4 LPM HHO in a three-cylinder engine resulted in only a 1.6% increase.

One possible reason for the smaller improvement observed in this study is the use of a multi-cylinder engine, which distributes the HHO mixture differently compared to the single-cylinder setups used in previous research.

Table 4. Comparison between the Present Study and Some of the Previous Studies

Flowrate HHO (LPM)	Cylinder	Thermal Efficiency	SFC/ BSEC	
0.5	1	Increase 8%	Decrease 9%	
11	1	Increase 25%	Decrease 92.27%	
0.2	1	Increase 47.24%	Decrease 32.1%	
3	4	Increase 6.55%	Decrease 7.85%	
0.4	3	Increase 1.6%	Decrease 3%	
	0.5 11 0.2 3	0.5 1 11 1 0.2 1 3 4	HHO (LPM) Cylinder Efficiency 0.5 1 Increase 8% 11 1 Increase 25% 0.2 1 Increase 47.24% 3 4 Increase 6.55% 0.4 3 Increase	

Additionally, the lower HHO flow rate (0.4 LPM) may have contributed to the more moderate enhancement in engine performance.

Despite the modest improvements, this study demonstrates that even at lower HHO flow rates, positive effects on engine performance can still be achieved. This is particularly significant for practical applications, where using less HHO offers a more sustainable and cost-effective approach to improving fuel efficiency and reducing emissions.

CONCLUSION

This experiment demonstrates that HHO blending enhances brake power, improves thermal efficiency, and reduces fossil fuel consumption under controlled load conditions. The findings highlight its potential as a practical and viable solution for reducing fossil fuel consumption in daily applications. The key results obtained are as follows:

1. Effect of KOH Molarity on Electrical Power Consumption

The results show a decreasing trend in electrical power consumption as KOH molarity increases. The lowest power consumption across all variations of current strength and KOH molarity was observed at a KOH concentration of 30% wt.

2. Effect of HHO Blending on Engine Performance

HHO blending in the combustion chamber led to improved engine performance. The optimal performance was achieved at an HHO flow rate of 0.4 L/min, resulting in a 4.9% increase in brake power, a 1.6% improvement in thermal efficiency, and a 3% reduction in brake-specific energy consumption.

ACKNOWLEDGMENT

The authors gratefully acknowledge the generous financial support given by the DIPA LPPM through the RIPEKDOM Scheme - in accordance with the Fiscal Year 2024 Research Contract University of Riau of Contract Number: 942/UN19.5.1.3/AL.04/2024.

REFERENCE

- [1] Md. M. Islam et al., "Response of Indonesian mineral supply to global renewable energy generation: Analysis based on gravity modelapproach," *Geoscience Frontiers*, p. 101658, Jun. 2023, doi: 10.1016/j.gsf.2023.10 1658.
- [2] A. Martin, Y. R. Ginting, I. Kurniawan, D. R. Agusta, and N. Khotimah, "Production of biocoal based on empty fruit bunches by torrefaction method with fixed bed and

- tubular continuous reactors," *SINERGI*, vol. 28, no. 2, p. 259, Apr. 2024, doi: 10.22441/sinergi.2024.2.006.
- [3] A. Martin, R. Hartono, and R. Asrian, "Utilizing waste heat gasoline engine in the design and fabrication of a fin and tube evaporator for the Organic Rankine Cycle (ORC)," SINERGI, vol. 27, no. 2, p. 171, Apr. 2023, doi:10.22441/sinergi. 2023. 2.004.
- [4] K. Ali, D. Jianguo, D. Kirikkaleli, G. Mentel, and M. Altuntaş, "Testing the role of digital financial inclusion in energy transition and diversification towards COP26 targets and sustainable development goals," *Gondwana Research*, vol. 121, pp. 293–306, Sep. 2023, doi: 10.1016/j.gr.2023. 05.006.
- [5] Z. Zikri et al., "Study on the production of hydrogen gas from water electrolysis on motorcycle engine," *J Mech. Elec. Pow., Vehi. Tech.,* vol. 13, no. 1, pp. 88–94, Jul. 2022, doi: 10.14203/j.mev.2022.v13.88-94.
- [6] Nasruddin, A. Martin, M. I. Alhamid, and D. Tampubolon, "Adsorption Isotherms of Hydrogen on Granular Activated Carbon Derived from Coal and Derived from Coconut Shell," *Heat Tran. Eng.*, vol. 38, no.4, pp.403–408, Mar. 2017, doi: 10.1080/01457632.2016.1194703.
- [7] A. A. Ingle, "Oxy Hydrogen Gas Generator Design and Development for SI Engine," vol.08, no. 10, pp.1691–1701, Oct. 2021.
- [8] F. Musy et al., "Hydrogen-fuelled internal combustion engines: Direct Injection versus Port-Fuel Injection," *Int J Hydrogen Energy*, Jul. 2024, doi: 10.1016/j.ijhydene.2024. 07.136.
- [9] M. Noussan et al., "The Role of Green and Blue Hydrogen in the Energy Transition-A Technological and Geopolitical Perspective," *Sustainability*, vol. 13, no. 1, p. 298, Dec. 2020, doi:10.3390/su 13010298.
- [10] M. Newborough and G. Cooley, "Developments in the global hydrogen market: The spectrum of hydrogen colours," Fuel Cells Bulletin, vol. 2020, no. 11, pp. 16– 22, Nov. 2020, doi: 10.1016/ S1464-2859(20)30546-0.
- [11] S. Shiva Kumar and V. Himabindu, "Hydrogen production by PEM water electrolysis A review," *Mater Sci Energy Technol*, vol. 2, no. 3, pp. 442–454, Dec. 2019, doi:10.1016/j.mset. 2019.03.002.
- [12] Anton Ottosson, "Integration of Hydrogen Production via Water Electrolysis at a CHP Plant," Luleå University of Technology, Norrbotten County, 2021.

- [13] F. Gambou et al., "A Comprehensive Survey of Alkaline Electrolyzer Modeling: Electrical Domain and Specific Electrolyte Conductivity," *Energies (Basel)*, vol. 15, no. 9, p. 3452, May 2022, doi: 10.3390/en15093452.
- [14] D. Choi and K.-Y. Lee, "Experimental Study on Water Electrolysis Using Cellulose Nanofluid," *Fluids*, vol. 5, no. 4, p. 166, Sep. 2020, doi: 10.3390/fluids 5040166.
- [15] F. Salek, M. Zamen, and S. V. Hosseini, "Experimental study, energy assessment and improvement of hydroxy generator coupled with a gasoline engine," *Energy Reports*, vol. 6, pp. 146–156, Nov. 2020, doi: 10.1016/j.egyr.2019.12.009.
- [16] L. Wang et al., "Review on blended hydrogen-fuel internal combustion engines: A case study for China," *Energy Reports*, vol. 8, pp. 6480–6498, Nov. 2022, doi: 10.1016/ j.egyr.2022.04.079.
- [17] L. V. Amaral et al., "Combustion and specific fuel consumption evaluation of a single-cylinder engine fueled with ethanol, gasoline, and a hydrogen-rich mixture," *Case Studies Therm Engi* vol. 57, p. 104316, May 2024, doi: 10.1016/j. csite.2024.104316.
- [18] M. Arana et al., "Acoustic and psychoacoustic levels from an internal combustion engine fueled by hydrogen vs. gasoline," *Fuel*, vol. 317, p. 123505, Jun. 2022, doi: 10.1016/j.fuel.2022.123505.
- [19] M. S. Gad et al., "Impact of produced oxyhydrogen gas (HHO) from dry cell electrolyzer on spark ignition engine characteristics," *Int. J .Hydrogen Energy*, vol. 49, pp. 553–563, Jan. 2024, doi: 10.1016/j.ijhydene.2023.08.210.
- [20] S. T. P. Purayil, S. Al-Omari, and E. Elnajjar, "Effect of hydrogen blending on the combustion performance, emission, and cycle-to-cycle variation characteristics of a single-cylinder GDI spark ignition dual-fuel engine," *Int. J. Thermo.*, vol. 20, p. 100403, Nov. 2023, doi: 10.1016/j.ijft.2023.100403.
- [21] H. Hassan et al., "Enhancement of the performance and emissions reduction of a hydroxygen-blended gasoline engine using different catalysts," *Appl Energy*, vol. 326, p. 119979, 2022, doi: doi.org/10.1016/ j.apenergy.2022.119979.
- [22] W. M. Adaileh and K. S. AlQdah, "Performance improvement and emission reduction of gasoline engine by adding hydrogen gas into the intake manifold," *Mater Today Proc*, vol. 60, pp. 1769–1778, 2022, doi:10.1016/j. matpr.2021.12.314.

- [23] M. Assad and Penazkov, "Comprehensive analysis of the operation of an internal combustion engine fueled by hydrogencontaining mixtures," *Energy Reports*, vol.9, pp. 4478–4492, Dec. 2023, doi: 10.1016/j.egyr. 2023.03.101.
- [24] C. E. Rustana *et al.*, "The Effect of Voltage and Electrode Types on Hydrogen Production from The Seawater Electrolysis Process," *J Phys Conf Ser*, vol. 2019, no. 1, p. 012096, Oct. 2021, doi: 10.1088/1742-6596/2019/1/012096.
- [25] S. Wang, A. Lu, and C.-J. Zhong, "Hydrogen production from water electrolysis: role of catalysts," *Nano Conver.*, vol. 8, no. 1, p. 4, Dec. 2021, doi: 10.1186/s40580-021-00254x.
- [26] A. W. Sari, A. Martin, and M. Habibillah, "Design of Wet Cell Type Hydrogen Electrolyzer Using Distilled Water as Raw Material," in 2024 4th International Conference on Electrical Engineering and Informatics (ICon EEI), Oct. 2024, pp. 17–21. doi:10.1109/IConEEI64414. 2024.10748096.
- [27] F. Gambou et al., "A Comprehensive Survey of Alkaline Electrolyzer Modeling: Electrical Domain and Specific Electrolyte Conductivity," *Energies (Basel)*, vol. 15, no. 9, p. 3452, May 2022, doi: 10.3390 /en15093452.
- [28] T. Nabil and M. M. Khairat Dawood, "Enabling efficient use of oxy-hydrogen gas (HHO) in selected engineering applications; transportation and sustainable power generation," *J. Clean. Prod.*, vol. 237, p. 117798, Nov. 2019, doi: 10.1016/j.jclepro.2019.117798.
- [29] Injection Technologies and Mixture Formation Strategies for Spark-Ignition and Dual-Fuel Engines. SAE International, 2022. doi: 10.4271/9781468603125.
- [30] M. R. Lad et al., "Development of Medium Duty H2 ICE for ON & OFF Highway Application," SAE Technical Paper, Jan. 2024. doi: 10.4271/2024-26-0170.
- [31] M. Mohamed et al., "Experimental investigation for enhancing the performance of hydrogen direct injection compared to gasoline in spark ignition engine through valve timings and overlap optimization," *Fuel*, vol. 372, p. 132257, 2024, doi: 10.1016/j.fuel.2024.132257